



HAL
open science

Uniform Sampling and Reconstruction of Trivariate Functions

Alireza Entezari

► **To cite this version:**

Alireza Entezari. Uniform Sampling and Reconstruction of Trivariate Functions. SAMPTA'09, May 2009, Marseille, France. pp.General session. hal-00453078

HAL Id: hal-00453078

<https://hal.science/hal-00453078>

Submitted on 3 Feb 2010

HAL is a multi-disciplinary open access archive for the deposit and dissemination of scientific research documents, whether they are published or not. The documents may come from teaching and research institutions in France or abroad, or from public or private research centers.

L'archive ouverte pluridisciplinaire **HAL**, est destinée au dépôt et à la diffusion de documents scientifiques de niveau recherche, publiés ou non, émanant des établissements d'enseignement et de recherche français ou étrangers, des laboratoires publics ou privés.

Uniform Sampling and Reconstruction of Trivariate Functions

Alireza Entezari

E301 CSE Building, University of Florida, Gainesville, FL, USA.
entezari@cise.ufl.edu

Abstract:

The Body Centered Cubic (BCC) and Face Centered Cubic (FCC) lattices have been known to outperform the commonly-used Cartesian sampling lattice due to their improved spectral sphere packing properties. However, the Cartesian lattice has been widely used for sampling of trivariate functions with applications in areas such as biomedical imaging, scientific data visualization and computer graphics. The widespread use of Cartesian lattice is partly due to the availability of tensor-product approach that readily extend the univariate reconstruction methods to trivariate setting. In this paper we report on recent advances on non-separable reconstruction algorithms, based on box splines, for reconstruction of data sampled on the BCC and FCC lattices. It turns out that these box spline reconstructions are *faster* than the corresponding tensor-product B-spline reconstructions on the Cartesian lattice. This suggests that not only the BCC and FCC lattices are more accurate sampling patterns, their respective reconstruction methods are also more computationally efficient than the tensor-product reconstructions – a fact which is contrary to the common assumption among practitioners.

1. Introduction

Sampling and reconstruction play a vital role in visualization and computer graphics. Various volume rendering algorithms rely on accurate reconstruction as a key step since the quality and fidelity of the rendered image heavily depends on reconstruction. In image processing reconstruction is used in resampling, resizing, conversion, and manipulation of sampled data.

In the realm of sampling, the term **regular** is often used to refer to the case that the sampling grid is uniform. Although there has been significant research, recently, in non-uniform sampling (e.g., sparse sampling, compressed sensing), the regular sampling is the most commonly-used sampling scheme in practice [21].

When it comes to sampling multivariate functions, the tensor-product of uniform sampling, which forms a Cartesian lattice, is almost always the choice. The simple structure of the Cartesian lattice and its separable nature allows one to readily apply a tensor-product paradigm to many problems in a multi-dimensional setting. The power of the dimensionality reduction will remain the major reason that the Cartesian lattice is the preferred tool in numerical

algorithms. The other attraction of the Cartesian lattice is that it simply exists in *any* dimension and often tools and theory extend to problems in a higher dimensional setting in a trivial manner.

However, the Cartesian lattice has been known to be an inefficient lattice from the sampling-theoretic point of view. Miyakawa [12] and then Petersen and Middleton [16] were among the first people to discover the superiority of sphere-packing and sphere-covering lattices for sampling multivariate functions. In particular they have demonstrated that Cartesian lattice is very inefficient for sampling multivariate functions.

2. Optimal Sampling Lattices

When sampling a multivariate function with a lattice, generated by (integer linear combinations of the columns of) a **sampling matrix**, M , the spectrum of the signal is contained in the **Brillouin zone**. Brillouin zone is the Voronoi cell of the **reciprocal** lattice. The reciprocal lattice to the lattice M is generated by the columns of the matrix $2\pi M^{-T}$. The multivariate version of the Nyquist frequency is the boundary of the Brillouin zone.

Without a priori knowledge when sampling multivariate functions, one often assumes that the underlying function has features possibly in all directions. Therefore, without knowledge about particular orientations of high-frequency features, we need to capture an *isotropic* spectrum during the sampling process. Therefore, the objective of optimal sampling is to maximize the isotropic content of the Brillouin zone. In other words, the sampling lattice whose Brillouin zone has the largest inscribing (hyper) sphere is the best sampling lattice. Therefore, the optimal sampling lattice in any dimension is the lattice whose reciprocal lattice allows for the densest packing of spheres.

In the bivariate setting the hexagonal lattice is the best sampling lattice since its reciprocal lattice, which happens to be the dual hexagonal lattice, allows for the best packing of 2-D with disks. When compared to the commonly-used Cartesian lattice with the same sampling density, the hexagonal lattice allows for about 14% more information to be captured in the spectrum of the underlying signal. This is illustrated in Figure 1 as the area of inscribing disc to the Brillouin zone of the hexagonal lattice (i.e., hexagon) is larger than the area of inscribing disc to the Brillouin zone of the Cartesian lattice (i.e., square), even

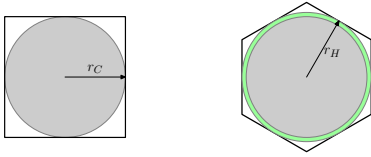


Figure 1: A square and a hexagon with unit area corresponding to the Brillouin zone of Cartesian and hexagonal sampling. The area of inscribing disk to a square is about 14% less than the area of the inscribing disk to the hexagon.

though the two Brillouin zones have the same area.

In the trivariate setting, the optimal sampling lattice is the BCC lattice whose reciprocal lattice (i.e., the FCC lattice) is the densest sphere packing lattice. The sampling efficiency of the BCC lattice, when compared to the commonly-used Cartesian lattice is about 30% higher. Appendix A in [6] presents a thorough comparison of the Brillouin zone of the Cartesian, BCC and FCC lattices.

The FCC lattice, is also superior to the Cartesian lattice as its efficiency compared to the Cartesian lattice is about 27% higher. Although among the FCC and BCC lattices the BCC wins, by a small margin, for optimal sampling, the FCC lattice appears to have good resistance to aliasing. This can be justified since its reciprocal lattice (i.e., the BCC lattice) allows for the best sphere covering of the space. The best covering of the space translates to replication of isotropic spectrum with minimal overlap between them— minimizing the aliasing for that sampling resolution.

These facts about comparison of the Cartesian, BCC and FCC lattices together with their higher-dimensional counter parts are discussed for sampling stationary isotropic random processes [10]. The arguments of the optimal sampling (BCC) and resilience to aliasing (FCC) is generalized to the notion that the reciprocal lattice for optimal sphere-packing lattice is the best choice for sampling functions at relatively high resolutions, while the sphere-packing lattice is the best option for sampling functions at relatively low resolutions [10].

3. Reconstruction

There is abundant research on reconstruction (i.e., interpolation or approximation) of data based on univariate filtering methods [15]. Various 1-D filters have a low-pass behavior and approximate the ideal kernel (i.e., sinc) for reconstruction into the space of band-limited functions. B-splines, offer a framework for representation of piecewise polynomial functions and thus are widely used in reconstruction of univariate functions [3].

There are two common methods for extending the univariate reconstruction ‘kernels’ to multivariate setting. The **separable** approach builds the multivariate kernel by a simple tensor-product of univariate kernels. The separable approach is obviously suitable for reconstruction of data on the Cartesian lattice since the lattice itself is also separable. The **radial** basis approaches construct the multivariate reconstruction kernel by spherical extension of

univariate kernel. Due to the spherical extension, the radial basis approach ignores the underlying geometry of the sampling lattice and is often used for scattered data interpolation/approximation.

Splines have been widely accepted for image processing [20]. In the context of image processing, splines are often constructed as a tensor-product of two univariate splines. Mitchell and Netravali [11], demonstrated the advantages of using splines for image processing. Recently, Van De Ville [22], developed the so called Hex-splines that are used for reconstruction of hexagonal images. Hex-splines can not be constructed as a tensor-product of univariate splines. Due to the non-separable structure of hexagonal lattice, the tensor-product splines can not be applied for processing of hexagonal data.

3.1 Reconstruction of trivariate functions

In the visualization community reconstruction filters have received a lot of attention since accurate reconstruction of trivariate functions and their gradients is crucial in fidelity of rendering algorithms [14, 1, 5, 13]. Similar to image processing, in volume visualization algorithms, often the tensor-product approach is used for reconstruction of Cartesian sampled data.

Theußl [18] introduced the BCC sampling in volume rendering. However, since the BCC lattice is a non-separable lattice, various ad-hoc tensor-product [17] and radial basis [18] algorithms fail to provide satisfactory reconstruction algorithms and they exhibit blurry artifacts. Csébfalvi [2] proposed a global pre-processing algorithm (based on generalized interpolation [19]) that reconstructs the BCC lattice based on its two Cartesian sub-lattices. This approach is computationally inefficient and does not guarantee approximation order.

The author’s recent work in this area establishes the relationship between box splines and the above-mentioned sampling lattices. The box splines have been developed as a generalization of B-splines to the multivariate setting. While box splines have been considered as non-separable basis functions for approximation based on their shifts on the Cartesian lattice [4], here their shifts on BCC and FCC lattices are considered. The interesting fact about these box splines is that while their shifts on the Cartesian lattice do not form a linearly independent set of functions, their shifts on the FCC and BCC lattices are linearly independent – a rare and useful property for the spline space!

3.2 Four direction box splines on BCC

The relation of box splines with the BCC lattice was established based on the fact that the immediate neighborhood of a lattice point on the BCC pattern forms a rhombic dodecahedron (see Figure 2). This polyhedron has the special property that is a projection of a four-dimensional hypercube (tesseract). This makes it a perfect match to be the support of a box spline since the geometric definition of box splines precisely amounts to projecting hypercubes (i.e., box) down to lower dimensional spaces. Generally, the class of polytopes that are the shadow of higher dimensional hypercubes are referred to as **zonotopes**. This linear box spline is defined by the four direction and is

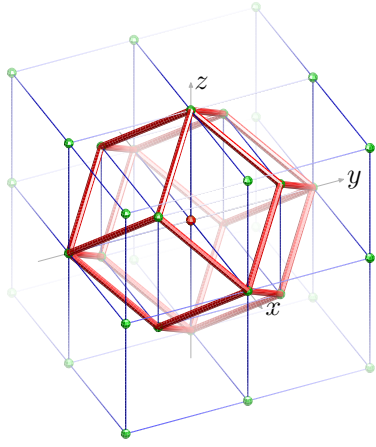


Figure 2: The neighborhood of a BCC lattice point forms a rhombic dodecahedron. This polyhedron is a zonohedron which is the support of a linear box spline.

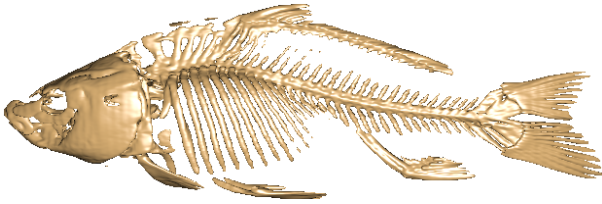


Figure 3: Benchmark example dataset. The CT dataset of a carp fish at a high resolution of $256 \times 256 \times 256$.

a C^0 kernel. The shifts of this box spline on the BCC lattice generate a spline space whose approximation order is two. By convolving this box spline by itself, one obtains a smoother, C^2 , quintic box spline that is specified by a repetition of the four principal directions. The shifts of this box spline generate a spline space whose approximation order is four [7, 8]. This smoothness and approximation order match that of the tricubic B-spline on the Cartesian lattice and hence we compare the two on a Carp fish dataset in first row in Figure 4. The piecewise polynomial representation of these box splines along with efficient evaluation methods can be found in [8].

3.3 The six direction box spline on FCC

Unlike the BCC lattice, the immediate neighborhood in the FCC lattice is not a zonohedron. However, by enlarging the neighborhood one finds the truncated octahedron which is a zonohedron Figure 5. This polyhedron is a projection of a six-dimensional hypercube and the corresponding box spline is a cubic six-direction box spline [6]. The spline space that is generated by shifts of this cubic box spline on the FCC lattice is a C^1 space whose approximation order is three. These characteristics match the triquadratic B-spline on the Cartesian lattice which is the base for our comparisons in second row in Figure 4. The piecewise polynomial representation of the cubic box spline along with efficient spline evaluation method on the FCC lattice is demonstrated in [9].

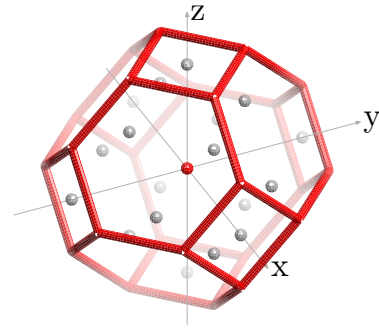


Figure 5: The neighborhood of a FCC lattice point forms a truncated octahedron. This polyhedron is another zonohedron which is the support of a six-direction box spline.

3.4 Computational advantages

Once efficient evaluation algorithms are derived for the four-direction box splines [8] and the six direction box spline [9], one can compare these box spline reconstructions to the commonly-used tensor-product B-spline reconstructions on the Cartesian lattice.

For the C^2 , fourth-order method the tricubic B-spline uses a neighborhood of $4 \times 4 \times 4 = 64$ points for reconstruction, while the quintic box spline only uses a total of 32 points for reconstruction. Therefore as documented in [8] the BCC non-separable box spline approach outperforms the comparable tensor-product B-spline approach by a factor of **two**. Similarly the triquadratic B-spline uses a neighborhood of $3 \times 3 \times 3 = 27$ Cartesian data points, while the cubic box spline only requires a total of 16 FCC data points for the reconstruction. Therefore, the non-separable box spline reconstruction outperforms the comparable tensor-product B-spline approach as documented in [9].

4. Conclusions

The recent research on optimal sampling lattices suggests that not only the FCC and BCC lattices offer higher-fidelity sampling schemes, but also their reconstruction algorithms outperform the corresponding tensor-product reconstructions on the traditionally-popular Cartesian lattice. These encouraging results are crucial for acceptance of these efficient lattices in practical applications.

5. Acknowledgments

The author would like to thank Dimitri Van De Ville, Torsten Möller and Carl de Boor for valuable insight and advice at various stages of the work.

References:

- [1] I. Carlbom. Optimal Filter Design for Volume Reconstruction and Visualization. In *Proc. IEEE Conf on Visualization*, pages 54–61, October 1993.
- [2] B. Cséfalvi. Prefiltered gaussian reconstruction for high-quality rendering of volumetric data sampled

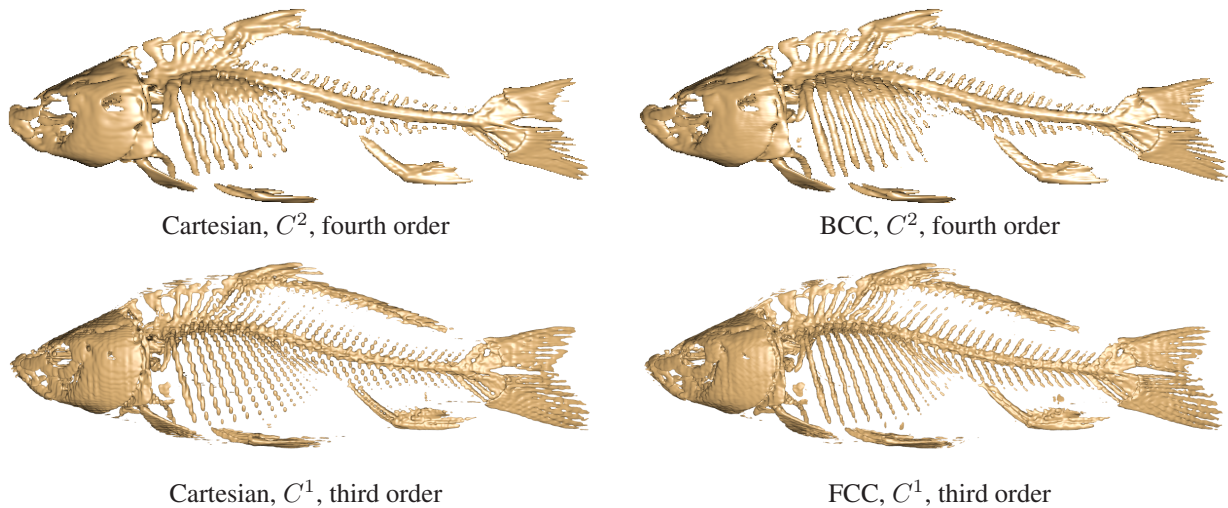


Figure 4: The Carp dataset at 6% resolution on Cartesian, BCC and FCC subsampled from the ground truth volume data of Figure 3. Top row: the Cartesian dataset is reconstructed by the tricubic B-spline and the BCC dataset is reconstructed by the quintic box spline. Bottom row: the Cartesian dataset is reconstructed with the triquadratic B-spline, while the FCC dataset is reconstructed with the cubic box spline. Superiority of the FCC and the BCC sampling is demonstrated since their images offer more accurate reconstruction than the Cartesian specially on the ribs and tail area.

- on a body-centered cubic grid. In *IEEE Visualization*, pages 311–318, 2005.
- [3] C. de Boor. *A practical guide to splines*, volume 27 of *Applied Mathematical Sciences*. Springer-Verlag, New York, revised edition, 2001.
 - [4] C. de Boor, K. Höllig, and S. Riemenschneider. *Box Splines*. Springer Verlag, 1993.
 - [5] S. C. Dutta Roy and B. Kumar. *Handbook of Statistics*, volume 10, chapter Digital Differentiators, pages 159–205. Elsevier Science Publishers B. V., N. Holland, 1993.
 - [6] A. Entezari. *Optimal Sampling Lattices and Trivariate Box Splines*. PhD thesis, Simon Fraser University, Vancouver, Canada, July 2007.
 - [7] A. Entezari, R. Dyer, and T. Möller. Linear and Cubic Box Splines for the Body Centered Cubic Lattice. In *Proceedings of the IEEE Conference on Visualization*, pages 11–18, October 2004.
 - [8] A. Entezari, D. Van De Ville, and T. Möller. Practical box splines for volume rendering on the body centered cubic lattice. *IEEE Trans. on Visualization and Comp Graphics*, 14(2):313 – 328, 2008.
 - [9] M. Kim, A. Entezari, and J. Peters. Box Spline Reconstruction on the Face Centered Cubic Lattice. *IEEE Trans. on Visualization and Computer Graphics*, 14(6):1523–1530, 2008.
 - [10] HR Kunsch, E. Agrell, and FA Hamprecht. Optimal lattices for sampling. *Information Theory, IEEE Transactions on*, 51(2):634–647, 2005.
 - [11] D. P. Mitchell and A. N. Netravali. Reconstruction Filters in Computer Graphics. In *Computer Graphics (Proceedings of SIGGRAPH 88)*, volume 22, pages 221–228, August 1988.
 - [12] H. Miyakawa. Sampling theorem of stationary stochastic variables in multidimensional space. *Journal of the Institute of Electronic and Communication Engineers of Japan*, 42:421–427, 1959.
 - [13] T. Möller, R. Machiraju, K. Mueller, and R. Yagel. A Comparison of Normal Estimation Schemes. In *Proceedings of the IEEE Conference on Visualization*, pages 19–26, October 1997.
 - [14] T. Möller, K. Mueller, Y. Kurzion, R. Machiraju, and R. Yagel. Design of Accurate and Smooth Filters for Function and Derivative Reconstruction. *Proceedings of the Symposium on Volume Visualization*, pages 143–151, Oct 1998.
 - [15] A.V. Oppenheim and R.W. Schaffer. *Discrete-Time Signal Processing*. Prentice Hall Inc., Englewoods Cliffs, NJ, 1989.
 - [16] D. P. Petersen and D. Middleton. Sampling and Reconstruction of Wave-Number-Limited Functions in N -Dimensional Euclidean Spaces. *Information and Control*, 5(4):279–323, December 1962.
 - [17] T. Theußl, O. Mattausch, T. Möller, and E. Gröller. Reconstruction schemes for high quality raycasting of the body-centered cubic grid. *TR-186-2-02-11, Institute of Computer Graphics and Algorithms, Vienna University of Technology*, December 2002.
 - [18] T. Theußl, T. Möller, and E. Gröller. Optimal Regular Volume Sampling. In *Proc of the IEEE Conf on Visualization*, pages 91–98, Oct 2001.
 - [19] P. Thévenaz, T. Blu, and M. Unser. Interpolation revisited. *IEEE Transactions on Medical Imaging*, 19(7):739–758, July 2000.
 - [20] M. Unser. Splines: A perfect fit for signal and image processing. *IEEE Signal Processing Magazine*, 16(6):22–38, November 1999. IEEE Signal Processing Society’s 2000 magazine award.
 - [21] M. Unser. Sampling—50 Years after Shannon. *Proceedings of the IEEE*, 88(4):569–587, April 2000.
 - [22] D. Van De Ville, T. Blu, M. Unser, W. Philips, I. Lemahieu, and R. Van de Walle. Hex-Splines: A Novel Spline Family for Hexagonal Lattices. *IEEE Trans. on Img Proc.*, 13(6):758–772, June 2004.